

Fast Exact Leverage Score Sampling from Khatri-Rao Products with Applications to Tensor Decomposition

Vivek Bharadwaj¹ Osman Asif Malik² Riley Murray^{3,2,1} Laura Grigori⁴ Aydın Buluç^{1,2} James Demmel¹

Abstract

We present a data structure to randomly sample rows from the Khatri-Rao product of several matrices according to the exact distribution of its leverage scores. Our proposed sampler draws each row in time logarithmic in the height of the Khatri-Rao product and quadratic in its column count, with persistent space overhead at most the size of the input matrices. As a result, it tractably draws samples even when the matrices forming the Khatri-Rao product have tens of millions of rows each. When used to sketch the linear least-squares problems arising in Candecomp / PARAFAC decomposition, our method achieves lower asymptotic complexity per solve than recent state-of-the-art methods. Experiments on billion-scale sparse tensors and synthetic data validate our theoretical claims, with our algorithm achieving higher accuracy than competing methods as the decomposition rank grows.

1. Introduction

The Khatri-Rao product (KRP, denoted \odot) is the column-wise Kronecker product of two matrices, and it appears in diverse applications across numerical analysis and machine learning. It features prominently in the alternating least squares (ALS) algorithm to compute the Candecomp / Parafac (CP) decomposition, which generalizes the matrix singular value decomposition to higher dimensions (Kolda & Bader, 2009). It also appears in second-order gradient descent methods, where it is used to approximate the Fisher information matrix of a neural network (Martens & Grosse, 2015). Many applications involve overdetermined least-squares problems of the form $\min_X \|AX - B\|_F$, where

¹EECS Department, UC Berkeley, CA, USA ²CRD, Lawrence Berkeley National Laboratory, CA, USA ³International Computer Science Institute, CA, USA ⁴Sorbonne Université, Inria, CNRS, Université de Paris, Laboratoire Jacques-Louis Lions, Paris, France. Correspondence to: James Demmel <demmel@berkeley.edu>.

the design matrix $A = U_1 \odot \dots \odot U_N$ is the Khatri-Rao product of matrices $U_j \in \mathbb{R}^{|I_j| \times R}$. In this work, we focus on the case where A has moderate column count (a few hundred at most). Despite this, traditional least-squares techniques such as QR decomposition are too slow because the height of A is $\prod_{j=1}^N |I_j|$. For row counts $|I_j|$ in the millions, it is intractable to even materialize A explicitly.

Several recently-proposed randomized sketching algorithms can approximately solve least squares problems with Khatri-Rao product design matrices (Jin et al., 2020; Larsen & Kolda, 2022; Malik et al., 2022). These methods apply a sketching operator S to the design and data matrices to solve the reduced least-squares problem $\min_{\tilde{X}} \|SA\tilde{X} - SB\|_F$, where S has far fewer rows than columns. For appropriately chosen S , the residual of the downsampled system falls within a specified tolerance ε of the optimal residual with high probability $1 - \delta$. In this work, we constrain S to be a *sampling matrix* that selects and reweights a subset of rows from both A and B . When the rows are selected according to the distribution of *statistical leverage scores* on the design matrix A , only $O(R/(\varepsilon\delta))$ samples are required. The challenge, then, is to efficiently sample according to the leverage scores when A has Khatri-Rao structure.

We propose a leverage-score sampler for the Khatri-Rao product of matrices with tens of millions of rows each. After construction, our sampler draws each row in time quadratic in the column count, but logarithmic in the height of the Khatri-Rao product. Our core contribution is the following theorem.

Theorem 1.1 (Efficient KRP Leverage Sampling). *Given U_1, \dots, U_N with $U_j \in \mathbb{R}^{|I_j| \times R}$, there exists a data structure satisfying the following:*

1. *The data structure has construction time $O\left(\sum_{j=1}^N |I_j| R^2\right)$ and requires additional storage space $O\left(\sum_{j=1}^N |I_j| R\right)$. If matrix U_j changes, the data structure can be updated in time $O(|I_j| R^2)$.*
2. *The data structure produces J samples from the Khatri-Rao product $U_1 \odot \dots \odot U_N$ according to the exact*

leverage score distribution on its rows in time

$$O\left(NR^3 + J \sum_{k=1}^N (R^2 \log \max(|I_k|, R))\right)$$

using $O(NR^3)$ scratch space. The structure can also draw samples from the KRP of all matrices excluding U_j for any index j .

The efficient update property and ability to exclude one matrix are important in CP decomposition. Combined with error guarantees for leverage-score sampling, we achieve an algorithm for alternating least-squares CP decomposition with asymptotic complexity lower than several recent state-of-the-art methods. Table 1 compares our ALS complexity for dense tensor decomposition to prior works.

Our method provides the most practical benefit on sparse tensors with massive mode sizes. As a result, we test our sampler on sparse tensor CP decomposition via alternating least-squares. On the Amazon tensor with 1.8 billion nonzeros, our algorithm STS-CP achieves 5.7% higher fit for a rank 100 decomposition compared to competing method CP-ARLS-LEV, with only 2% higher average runtime at the same sample count. Even when CP-ARLS-LEV uses three times as many samples and 49% more runtime compared to STS-CP, STS-CP still exhibits 1.3% higher fit (see figure 8a in appendix A.8.3). Our method could be generalized to sample from structured matrices besides the Khatri-Rao product or used as a building block for more sophisticated sampling procedures based on determinantal point processes (Derezinski & Mahoney, 2021).

Table 1. Complexity of recent methods for N -dimensional dense tensor CP decomposition via alternating least squares. Factors involving $\log R$ and $\log(1/\delta)$ are hidden. See A.1 for details.

METHOD	COMPLEXITY PER ITERATION
CP-ALS	$N(N+I)I^{N-1}R$
CP-ARLS-LEV	$N(R+I)R^N/(\varepsilon\delta)$
TNS-CP	$N^3IR^3/(\varepsilon\delta)$
MA & SOLOMONIK 2022	$N^2(N^{1.5}R^{3.5}/\varepsilon^3 + IR^2)/\varepsilon^2$
STS-CP (OURS)	$N(NR^3 \log I + IR^2)/(\varepsilon\delta)$

2. Preliminaries and Related Work

Below, we use \otimes as the elementwise product of vectors / matrices, \cdot for matrix multiplication, and $\langle \cdot, \dots, \cdot \rangle$ as a generalized inner product. The latter operation returns the sum of all entries in the elementwise product of its arguments. We use Matlab notation $A[i, :]$, $A[:, i]$ to index rows, resp. columns, of matrices. For consistency, we use the convention that $A[i, :]$ is a row vector. Hence $A[i, :]^\top A[i, :]$

denotes an outer product, not an inner product. Finally, M^+ denotes the pseudoinverse of matrix M .

A variety of random sketching operators S have been proposed to solve overdetermined least-squares problems $\min_X \|AX - B\|_F$ when A has no special structure (Woodruff et al., 2014; Ailon & Chazelle, 2009). A few popular choices include *sampling* matrices, which have a single nonzero entry per row, operators composed of fast Fourier / trigonometric transforms, or Countsketch-type operators. Each sketch type can be adapted when A is a Khatri-Rao product (Cheng et al., 2016; Jin et al., 2020; Wang et al., 2015). For tensor decomposition, however, the matrix B may be sparse or implicitly specified as a black-box function. When B is sparse, Countsketch-type operators may still require the algorithm to iterate over all nonzero values in B in the worst case. As Larsen and Kolda note, operators similar to the FFT induce fill-in when applied to a sparse matrix B , destroying the benefits of sketching (2022). Similar difficulties arise when B is implicitly specified. This motivates our decision to focus on sampling operators, which only touch a subset of entries from B . Let $\hat{x}_1, \dots, \hat{x}_J$ be a selection of J indices for the rows of $A \in \mathbb{R}^{I \times R}$, sampled i.i.d. according to a probability distribution q_1, \dots, q_I . The associated sampling matrix $S \in \mathbb{R}^{J \times I}$ is specified by

$$S[i, j] = \begin{cases} \frac{1}{\sqrt{Jq_j}}, & \text{if } \hat{x}_i = j \\ 0, & \text{otherwise} \end{cases}$$

where the weight of each nonzero entry corrects bias induced by sampling. Among a variety of choices, the distribution q can be selected as uniform, proportional to the row norms of A , or according to the leverage scores of A . The latter has the strongest guarantee on solution quality (Derezinski & Mahoney, 2021).

2.1. Leverage Score Sampling Guarantees

The leverage scores of a matrix assign a measure of importance to each of its rows. The leverage score of row i from matrix $A \in \mathbb{R}^{I \times R}$ is given by

$$\ell_i = A[i, :] (A^\top A)^+ A[i, :]^\top \quad (1)$$

for $1 \leq i \leq I$. Leverage scores can be expressed equivalently as the squared row norms of the matrix Q in a reduced QR factorization of A (Drineas et al., 2012). By dividing the scores by the normalizing constant $C = \sum_{i=1}^I \ell_i$, we induce a probability distribution on the rows used to generate a sampling matrix S . The next theorem has appeared in several works, and we take the form given by Malik et al. (2022). For an appropriate sample count, it guarantees that the residual of the downsampled problem is close to the residual of the original problem.

Theorem 2.1 (Guarantees for Leverage Score Sampling). *Given $A \in \mathbb{R}^{I \times R}$ and $\varepsilon, \delta \in (0, 1)$, let $S \in \mathbb{R}^{J \times I}$*

be a leverage score sampling matrix for A . Further define $\tilde{X} = \operatorname{argmin}_X \|SAX - SB\|_F$. If $J \gtrsim R \max(\log(R/\delta), 1/(\varepsilon\delta))$, then with probability at least $1 - \delta$ it holds that

$$\|A\tilde{X} - B\|_F \leq (1 + \varepsilon) \min_X \|AX - B\|_F$$

For the applications considered in this work, R ranges up to a few hundred. As ε and δ tend to 0 with fixed R , $1/(\varepsilon\delta)$ dominates $\log(R/\delta)$. Hence, we assume that the minimum sample count J to achieve the guarantees of the theorem is $O(R/(\varepsilon\delta))$.

2.2. Prior Work on KRP Leverage Scores

Well-known sketching algorithms exist to quickly estimate the leverage scores of dense matrices (Drineas et al., 2012). These algorithms are, however, intractable for $A = U_1 \odot \dots \odot U_N$ due to the height of the Khatri-Rao product. Cheng et al. instead approximate each score as a product of leverage scores associated with each matrix U_j (2016). Larsen and Kolda propose CP-ARLS-LEV, which uses a similar approximation and combines random sampling with a deterministic selection of high-probability indices (2022). Both methods were presented in the context of CP decomposition. To sample from the KRP of N matrices, both require $O(R^N/(\varepsilon\delta))$ samples to achieve the (ε, δ) guarantee on the residual of each least-squares solution. These methods are simple to implement and perform well when the Khatri-Rao product has sufficiently low column count. On the other hand, they suffer from high sample complexity as R and N increase. The TNS-CP algorithm by Malik et al. samples from the exact leverage score distribution, thus requiring only $O(R/(\varepsilon\delta))$ samples per least-squares solve (2022). Unfortunately, it requires time $O(\sum_{j=1}^N |I_j| R^2)$ to draw each sample. Our goal is to preserve the low sample count of the latter approach, reduce the per-sample computation cost to logarithmic in $|I_j|$, and maintain space complexity linear in the input size (critical when the matrices U_j are tall).

3. An Efficient Khatri-Rao Leverage Sampler

Our algorithm will draw a single sample from the Khatri-Rao product by sampling a row from matrices U_1, U_2, \dots in succession and returning their elementwise product. The row from U_j is drawn conditioned on prior draws from U_1, \dots, U_{j-1} . Computing the full conditional distribution on the rows of U_j costs $O(|I_j| R^2)$ per sample, too costly when U_j has millions of rows. It is likewise intractable (in preprocessing time and space complexity) to precompute probabilities for every possible conditional distribution on the rows of U_j , since the conditioning random variable has

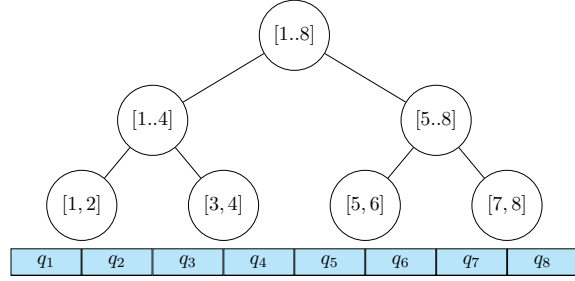


Figure 1. A segment tree $T_{8,2}$ and probability distribution $\{q_1, \dots, q_8\}$ on $[1, \dots, 8]$.

$\prod_{k=1}^{j-1} |I_k|$ potential values. The key to balancing sampling complexity with preprocessing time / space is to break the conditional distribution into a *mixture* of several components. We will select a component conditioned on prior draws with a modified binary search, only computing a few probabilities from the conditional distribution explicitly.

3.1. Segment Tree Sampling

Suppose we want to sample indices from the set $\{1..I\}$ according to a probability distribution $q = \{q_1, \dots, q_I\}$. When the probability vector q is known in advance and is the same for all samples, methods that draw each sample in constant time have long been known (Walker, 1974). In our case, however, each sample will be drawn from a potentially *unique* distribution q induced by a conditioning random variable. Instead, we consider an inversion sampling algorithm based on binary search (Saad et al., 2020). As a preprocessing step, this method divides the interval $[0, 1]$ into I bins, where the i 'th bin has endpoints $[\sum_{j=0}^{i-1} q_j, \sum_{j=0}^i q_j]$. For each sample, it draws a real number $D \sim \text{Uniform}(0, 1)$ and returns the index of the containing bin, located through a binary search on the list of endpoints. The preprocessing cost is $O(I)$ to compute the bin endpoints via a prefix sum, while the cost to draw each sample is $O(\log I)$.

Now consider the variation on the inversion sampling method presented in algorithm 1. This algorithm traverses a full, complete binary tree $T_{I,F} = \{v_1, v_2, \dots\}$ from root to leaf, where each node v is equipped with a nonempty, contiguous segment $S(v) = [S_0(v)..S_1(v)] \subseteq \{1..I\}$. We call $T_{I,F}$ a *segment tree*. We further require that the segments owned by the leaves partition $\{1..I\}$ and each have cardinality at most F . As illustrated in figure 1, the segment owned by each non-leaf v is the union of segments held by its children, $L(v)$ and $R(v)$.

Unlike standard inversion sampling, algorithm 1 does not access the bin endpoints directly. It takes two function arguments $\tilde{m} : T_{I,F} \rightarrow \mathbb{R}_+$ and $\tilde{q} : T_{I,F} \rightarrow \mathbb{R}_+^F$. The former determines the cutoff for branching left or right at each internal node, while the latter produces an F -length vector giving the width of each bin falling in the interval

Algorithm 1 STSample($T_{I,F}, \tilde{m}(\cdot), \tilde{q}(\cdot)$)

```

1:  $c := \text{root}(T_{I,F}), \text{low} = 0.0, \text{high} = 1.0$ 
2: Sample  $D \sim \text{Uniform}(0.0, 1.0)$ 
3: while  $c \notin \text{leaves}(T_{I,F})$  do
4:    $\text{cutoff} := \text{low} + \tilde{m}(L(c))$ 
5:   if  $\text{cutoff} \geq D$  then
6:      $c := L(c), \text{high} := \text{cutoff}$ 
7:   else
8:      $c := R(c), \text{low} := \text{cutoff}$ 
9:    $m_c := \tilde{m}(c)$ 
10: return  $S_0(v) + \text{argmin}_{i \geq 0} \left( \text{low} + \sum_{j=1}^i \tilde{q}(c)[j] < D \right)$ 

```

of a leaf. As the following simple proposition formalizes, appropriate choices for \tilde{m} and \tilde{q} allow the procedure in Algorithm 1 to sample from the distribution q .

Proposition 3.1 (Algorithm 1 Correctness). *For probability distribution $\{q_1, \dots, q_I\}$, suppose $\tilde{m}(v) = \sum_{i \in S(v)} q_i$ and $\tilde{q}(v) = \{q_i \mid i \in S(v)\}^1$. Then STSample($T_{I,F}, \tilde{m}, \tilde{q}$) returns index i with probability q_i .*

Proof. Setting \tilde{m} as specified by the proposition makes the loop starting on line 3 identical to a truncated binary search on the list of bin endpoints. The algorithm terminates the search when it reaches a leaf and the number of bins to search is at most F . Line 10 scans through all bin endpoints associated with the leaf (extracted from the function \tilde{q}) and returns the bin index containing D . Since bin i has width q_i and D was drawn uniformly from $[0, 1)$, the claim follows. \square

The depth of $T_{I,F}$ is $\lceil \log[I/F] \rceil$. Suppose now that we have procedures to compute $\tilde{m}(v)$ in time τ_1 for all $v \in T_{I,F}$ and $\tilde{q}(v)$ in time $\tau_2(F)$ for $v \in \text{leaves}(T_{I,F})$, where $\tau_2(F) \geq O(F)$. Then the runtime of STSample is

$$O(\tau_1 \lceil \log[I/F] \rceil + \tau_2(F)) \quad (2)$$

Thus, we require efficient functions $\tilde{m}(\cdot)$ and $\tilde{q}(\cdot)$ to achieve low sampling complexity.

3.2. A Simpler Row-Sampling Problem

As a building block for our efficient Khatri-Rao Product leverage-score sampler, we use Algorithm 1 to solve a simpler row-sampling problem. Consider the task of sampling J rows from a matrix $U \in \mathbb{R}^{I \times R}$. Let \hat{s} be the random variable for the index of a row sample, which takes on values in $\{1..I\}$. Further let $h \in \mathbb{R}^R, Y \in \mathbb{R}^{R \times R}$ be a vector and a positive semidefinite matrix, respectively. We will sample

¹If there are fewer than F elements in $S(v)$, the procedure $\tilde{q}(v)$ should pad its result with 0.

rows according to the following distribution on the rows of U :

$$\begin{aligned} p(\hat{s} = s \mid h, U, Y) &:= q_{h,U,Y}[s] \\ &:= C^{-1} \langle hh^\top, U[s, :]^\top U[s, :], Y \rangle \end{aligned} \quad (3)$$

where $C = \langle hh^\top, U^\top U, Y \rangle$, and provided C is nonzero². We impose that all J rows are drawn with the same matrices Y and U , but potentially distinct vectors h . To handle this, we use algorithm 1. For an internal node $v \in T_{I,F}$ in a segment tree on $\{1..I\}$, define function \tilde{m} (that depends implicitly on h, U , and Y) as

$$\begin{aligned} \tilde{m}(v) &:= \sum_{i \in S(v)} q_{h,U,Y}[i] \\ &= \sum_{i \in S(v)} C^{-1} \langle hh^\top, U[i, :]^\top U[i, :], Y \rangle \\ &= C^{-1} \langle hh^\top, \sum_{i \in S(v)} U[i, :]^\top U[i, :], Y \rangle \\ &:= C^{-1} \langle hh^\top, G^v, Y \rangle. \end{aligned} \quad (4)$$

Here, we define $G^v := \sum_{i \in S(v)} U[i, :]^\top U[i, :]$. We call each matrix G^v a *partial gram matrix*, since it is a sum of a subset of outer products required to form the complete gram matrix of U . If the partial gram matrices G^v are precomputed, then \tilde{m} is computable in time $O(R^2)$ from the last line of equation (4). Likewise, define the procedure \tilde{q} (which again depends on h, U , and Y implicitly) as

$$\begin{aligned} \tilde{q}(v) &:= \\ &C^{-1} \text{diag} \left(U[S(v), :] \cdot (hh^\top \otimes Y) \cdot U[S(v), :]^\top \right), \end{aligned} \quad (5)$$

which is computable in time $O(FR^2)$ when v is a leaf. Recalling that $S_0(v)$ is the beginning index of the segment held by a leaf v , we have for $i \in S(v)$

$$\begin{aligned} \tilde{q}(v)[i - S_0(v)] &= C^{-1} U[i, :] \cdot (hh^\top \otimes Y) \cdot U[i, :]^\top \\ &= C^{-1} \langle hh^\top, U[i, :]^\top U[i, :], Y \rangle \\ &= q_{h,U,Y}[i]. \end{aligned} \quad (6)$$

Then the functions \tilde{m} and \tilde{q} satisfy the requirements of proposition 3.1. Armed with these observations, we are ready to construct an efficient row sampler with properties detailed in the next lemma.

Lemma 3.2 (Efficient Row Sampler). *Given matrices $U \in \mathbb{R}^{I \times R}, Y \in \mathbb{R}^{R \times R}$ with Y p.s.d, there exists a data structure parameterized by positive integer F that satisfies the following:*

²If $C = 0$, impose $q_{h,U,Y}[s] = 1/I$ for all s , which is uniform and admits efficient sampling.

1. The structure has construction time $O(IR^2)$ and storage requirement $O(R^2\lceil I/F \rceil)$. If $I < F$, the storage requirement drops to $O(1)$.
2. After construction, the data structure can produce a sample according to the distribution $q_{h,U,Y}$ in time $O(R^2 \log\lceil I/F \rceil + FR^2)$ for any vector h .
3. If $Y = [1]$ (a matrix of all ones), the time per sample drops to $O(R^2 \log\lceil I/F \rceil + FR)$.

To construct the sampler, we compute and store the partial gram matrices G^v . The sampling phase calls the STSample procedure with appropriate functions \tilde{m} and \tilde{q} . Appendix A.2 gives a full proof of lemma 3.2. It also defines constructor “BuildSampler” and procedure “RowSample” for the claimed data structure, which we use in the next section.

3.3. Sampling from the Khatri-Rao Product

We will now use the row sampling lemma from section 3.2 twice in succession to assemble our Khatri-Rao leverage sampler and outline the proof of theorem 1.1. Without loss of generality, we prove part 2 of the theorem for the case where $A = U_1 \odot \dots \odot U_N$, as the case that excludes a single matrix from the KRP follows by reindexing matrices U_k . We also assume that A is a nonzero matrix. Let us index each row of A by a tuple $(i_1, \dots, i_N) \in I_1 \times \dots \times I_N$. Equation (1) gives

$$\begin{aligned} \ell_{i_1, \dots, i_N} \\ = A[(i_1, \dots, i_N), :] (A^\top A)^+ A[(i_1, \dots, i_N), :]^\top \end{aligned} \quad (7)$$

For $1 \leq k \leq N$, define $G_k := U_k^\top U_k$ and $G := \left(\bigotimes_{k=1}^N G_k\right)$; it is a well-known fact that $G = A^\top A$ (Kolda & Bader, 2009). For a single row sample from A , let $\hat{s}_1, \dots, \hat{s}_N$ be random variables for the draws from multi-index set $I_1 \times \dots \times I_N$ according to the leverage score distribution. Assume, for some k , that we have already sampled an index from each of I_1, \dots, I_{k-1} . This means that the first $k-1$ random variables take values $\hat{s}_1 = s_1, \dots, \hat{s}_{k-1} = s_{k-1}$, a condition we abbreviate as $\hat{s}_{<k} = s_{<k}$. To sample from I_k , we seek the distribution of \hat{s}_k conditioned on $\hat{s}_1, \dots, \hat{s}_{k-1}$. To simplify our equations, define $h_{<k}$ as the transposed elementwise product³ of rows already sampled:

$$h_{<k} := \left(\bigotimes_{i=1}^{k-1} U_i[s_i, :]\right)^\top. \quad (8)$$

³For $a > b$, assume that $\bigotimes_{i=a}^b (\dots)$ produces a vector / matrix filled with ones.

Also define $G_{>k}$ as

$$G_{>k} := G^+ \otimes \left(\bigotimes_{i=k+1}^N G_i\right). \quad (9)$$

Then the following theorem from Malik (adapted appropriately) gives the conditional distribution of \hat{s}_k .

Theorem 3.3 (Malik 2022, Adapted). *For any $s_k \in I_k$,*

$$\begin{aligned} p(\hat{s}_k = s_k \mid \hat{s}_{<k} = s_{<k}) \\ = C^{-1} \langle h_{<k} h_{<k}^\top, U_k[s_k, :]^\top U_k[s_k, :], G_{>k} \rangle \end{aligned} \quad (10)$$

where $C = \langle h_{<k} h_{<k}^\top, U_k^\top U_k, G_{>k} \rangle$ is nonzero.

We include the derivation of theorem 3.3 from equation (7) in appendix A.3. Notice that the conditional distribution is exactly $q_{h_{<k}, U_k, G_{>k}}$ as defined in section 3.2. While it is tempting to apply lemma 3.2 immediately, we take a longer path to achieve better time and space complexity.

Below, we abbreviate $q = q_{h_{<k}, U_k, G_{>k}}$ and $h = h_{<k}$. When sampling from I_k , observe that $G_{>k}$ is the same for all samples. We compute a symmetric eigendecomposition $G_{>k} = V\Lambda V^\top$, where each column of V is an eigenvector of $G_{>k}$. This allows us to rewrite entries of q as

$$\begin{aligned} q[s] &= C^{-1} \langle h h^\top, U_k[s, :]^\top U_k[s, :], G_{>k} \rangle \\ &= C^{-1} \langle h h^\top, U_k[s, :]^\top U_k[s, :], \sum_{u=1}^R \lambda_u V[:, u] V[:, u]^\top \rangle \\ &= C^{-1} \sum_{u=1}^R \lambda_u \langle h h^\top, U_k[s, :]^\top U_k[s, :], V[:, u] V[:, u]^\top \rangle. \end{aligned} \quad (11)$$

Define matrix $W \in \mathbb{R}^{|I_k| \times R}$ elementwise by

$$W[t, u] := \langle h h^\top, U_k[t, :]^\top U_k[t, :], V[:, u] V[:, u]^\top \rangle$$

and observe that all of its entries are nonnegative. Since $\lambda_u \geq 0$ for all u ($G_{>k}$ is p.s.d.), we can write q as a mixture of probability distributions given by the normalized⁴ columns of W :

$$q = \sum_{u=1}^R e[u] \frac{W[:, u]}{\|W[:, u]\|_1},$$

where the vector e of nonnegative weights is given by $e[u] = (C^{-1} \lambda_u \|W[:, u]\|_1)$. Rewriting q in this form allows us to break the sampling procedure into two phases: sampling a component of the mixture according to the weight vector e , then sampling an index in $\{1..|I_k|\}$ according to the p.m.f. defined by column $W[:, u]$. Let \hat{u}_k be a random variable distributed according to the probability

⁴Replace $W[:, u] / \|W[:, u]\|_1$ with a vector of 1’s when $\|W[:, u]\|_1 = 0$. This does not affect the calculation.

mass vector e . We have, for C taken from theorem 3.3 and a new normalizing constant B ,

$$\begin{aligned}
 p(\hat{u}_k = u_k) &= \frac{\lambda_{u_k}}{BC} \sum_{t=1}^{|I_k|} W[t, u_k] \\
 &= \frac{\lambda_{u_k}}{BC} \sum_{t=1}^{|I_k|} \langle hh^\top, U_k[t, :]^\top U_k[t, :], V[:, u_k] V[:, u_k]^\top \rangle \\
 &= \frac{\lambda_{u_k}}{BC} \langle hh^\top, \sum_{t=1}^{|I_k|} U_k[t, :]^\top U_k[t, :], V[:, u_k] V[:, u_k]^\top \rangle \\
 &= \frac{\lambda_{u_k}}{BC} \langle hh^\top, G_k, V[:, u_k] V[:, u_k]^\top \rangle \\
 &= q_{h, \sqrt{\Lambda} V^\top, G_k}[u_k].
 \end{aligned} \tag{12}$$

Hence, we can use the data structure in lemma 3.2 with $F = 1$ to sample a value for \hat{u}_k efficiently. Now introduce a random variable \hat{t}_k with distribution conditioned on \hat{u}_k given by

$$p(\hat{t}_k = t_k \mid \hat{u}_k = u_k) := W[t_k, u_k] / \|W[:, u_k]\|_1.$$

This distribution is well-defined, since we suppose that $\hat{u}_k = u_k$ occurs with nonzero probability $e[u_k]$, which implies that $\|W[:, u_k]\|_1 \neq 0$. Our remaining task is to efficiently sample from the distribution above. Below, we abbreviate $\tilde{h} = V[:, u_k] \otimes h$ and derive

$$\begin{aligned}
 p(\hat{t}_k = t_k \mid \hat{u}_k = u_k) &= \frac{\langle hh^\top, U_k[t_k, :]^\top U_k[t_k, :], V[:, u_k] V[:, u_k]^\top \rangle}{\|W[:, u_k]\|_1} \\
 &= \frac{\langle \tilde{h} \tilde{h}^\top, U_k[t_k, :]^\top U_k[t_k, :], [1] \rangle}{\|W[:, u_k]\|_1} \\
 &= q_{\tilde{h}, U_k, [1]}[t_k].
 \end{aligned} \tag{13}$$

Based on the last line of equation (13), we apply lemma 3.2 again to build an efficient sampling data structure parameterized by $F = R$ and $Y = [1]$. Since $Y = [1]$, our lemma yields an improved per-sample runtime.

To summarize, algorithms 2 and 3 give the construction and sampling procedures for our data structure. They rely on the ‘‘BuildSampler’’ and ‘‘RowSample’’ procedures from algorithms 4 and 5 in appendix A.2, which relate to the data structure in lemma 3.2. In the construction phase, we build N data structures from lemma 3.2 for the distribution in equation (13). Construction costs $O\left(\sum_{j=1}^N |I_j| R^2\right)$, and if any matrix U_j changes, we can rebuild Z_j in isolation. Because $F = R$, the space required for Z_j is $O(|I_j| R)$.

In the sampling phase, the procedure in algorithm 3 accepts an index j of a matrix to exclude from the Khatri-Rao product. This can be set to -1 to sample from the KRP of all

matrices. The procedure begins by computing the symmetric eigendecomposition of each matrix $G_{>k}$. It then creates data structures E_k for each of the distributions specified by equation (12). These data structures (along with those from the construction phase) are used to draw \hat{u}_k and \hat{t}_k in succession. The random variables \hat{t}_k follow the distribution in theorem 3.3 conditioned on prior draws, so the multi-index $(\hat{t}_k)_{k \neq j}$ follows the leverage score distribution on A . This completes a proof outline of theorem 1.1. Appendix A.4 proves the complexity claims in the theorem and provides a line-by-line analysis of the algorithms.

Algorithm 2 ConstructKRPSampler(U_1, \dots, U_N)

- 1: **for** $j = 1..N$ **do**
 - 2: $Z_j := \text{BuildSampler}(U_j, F = R, [1])$
 - 3: $G_j := U_j^\top U_j$
-

Algorithm 3 KRPSample(j, J)

- 1: $G := \bigotimes_{k \neq j} G_k$
 - 2: **for** $k \neq j$ **do**
 - 3: $G_{>k} := G^+ \otimes \bigotimes_{j+1}^N G_k$
 - 4: Decompose $G_{>k} = V_k \Lambda_k V_k^\top$
 - 5: $E_k := \text{BuildSampler}(\sqrt{\Lambda_k} \cdot V_k^\top, F = 1, G_k)$
 - 6: **for** $d = 1..J$ **do**
 - 7: $h = [1, \dots, 1]^\top$
 - 8: **for** $k \neq j$ **do**
 - 9: $\hat{u}_k := \text{RowSample}(E_k, h)$
 - 10: $\hat{t}_k := \text{RowSample}(Z_k, h \otimes (V_k[:, \hat{u}_k]))$
 - 11: $h * = U_k[\hat{t}_k, :]$
 - 12: $s_d = (\hat{t}_k)_{k \neq j}$
 - 13: **return** s_1, \dots, s_J
-

3.4. Application to Tensor Decomposition

A tensor is a multidimensional array, and the CP decomposition represents a tensor as a sum of outer products (Kolda & Bader, 2009). Alternating least-squares is one of the most popular iterative methods to compute a CP decomposition. To decompose an N -dimensional tensor \mathcal{T} , ALS begins with randomly initialized factor matrices U_1, \dots, U_N . Each round of ALS solves N overdetermined least-squares problems in sequence, each optimizing a single factor matrix while holding the others constant. The j 'th least-squares problem occurs in the update

$$U_j := \operatorname{argmin}_{U_j} \|U_{\neq j} \cdot U_j^\top - \operatorname{mat}(\mathcal{T}, j)\|_F \tag{14}$$

where $U_{\neq j}$ is the KRP of all matrices excluding U_j and $\operatorname{mat}(\cdot)$ denotes the mode- j matricization of tensor \mathcal{T} (see A.5 for a definition). These problems are ideal candidates for leverage-score sampling, and applying the data structure in theorem 1.1 gives us the **STS-CP** algorithm.

Corollary 3.4 (STS-CP). *Suppose \mathcal{T} is dense, and suppose we solve each least-squares problem in ALS with a*

randomized sketching algorithm. A leverage score sampling approach as defined in section 2 guarantees that with $O(R/(\varepsilon\delta))$ samples per solve, the residual of each sketched least-squares problem is within $(1 + \varepsilon)$ of the optimal residual with probability $(1 - \delta)$. The efficient sampler from theorem 1.1 brings the complexity of ALS to

$$O\left(\frac{\#it}{\varepsilon\delta} \cdot \sum_{j=1}^N (NR^3 \log |I_j| + |I_j| R^2)\right)$$

with any term $\log |I_j|$ replaced by $\log R$ if $|I_j| < R$.

The proof appears in appendix A.5 and combines theorem 1.1 with theorem 2.1. STS-CP also works for sparse tensors and likely provides a greater advantage here than the dense case, as sparse tensors tend to have much larger mode sizes. The complexity for sparse tensors depends heavily on the sparsity structure and is difficult to predict. Nevertheless, we expect a significant speedup based on prior works that use sketching to accelerate CP decomposition (Cheng et al., 2016; Larsen & Kolda, 2022).

4. Experiments

Experiments were conducted on CPU nodes of NERSC Perlmutter, and our code is available online⁵. On tensor decomposition experiments, we compare our algorithms against the random and hybrid versions of CP-ARLS-LEV proposed by Larsen and Kolda (2022). These algorithms outperform uniform sampling and row-norm-squared sampling, achieving excellent accuracy and runtime relative to exact ALS. In contrast to TNS-CP and the Gaussian tensor network embedding proposed by Ma and Solomonik (see table 1), CP-ARLS-LEV is one of the few algorithms that can practically decompose sparse tensors with mode sizes in the millions. In the worst case, CP-ARLS-LEV requires $O(R^{N-1}/(\varepsilon\delta))$ samples per solve for an N -dimensional tensor to achieve the (ε, δ) solution guarantee, compared to $O(R/(\varepsilon\delta))$ samples required by STS-CP. Appendices A.6 and A.7 provide further details about the experimental configuration and hybrid CP-ARLS-LEV.

4.1. Runtime Benchmark

Figure 2 shows the time to construct our sampler and draw 50,000 samples from the Khatri-Rao product of i.i.d. Gaussian initialized factor matrices. We quantify the runtime impacts of varying N , R , and I . The asymptotic behavior in theorem 1.1 is reflected in our performance measurements, with the exception of the plot that varies R . Here, construction becomes disproportionately cheaper than sampling due to cache-efficient BLAS3 calls during construction. Even

⁵https://github.com/vbharadwaj-bk/fast_tensor_leverage

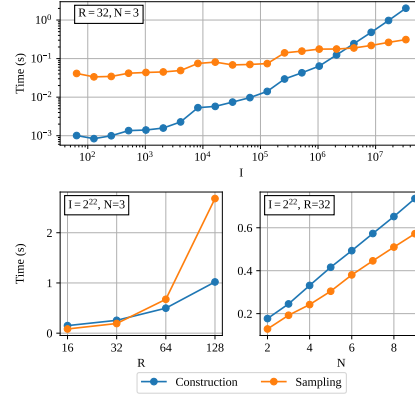


Figure 2. Time to construct our proposed sampler and draw $J = 50,000$ samples from the KRP of N i.i.d. random normal matrices $U_j \in \mathbb{R}^{I \times R}$. Each datapoint is an average of five measurements.

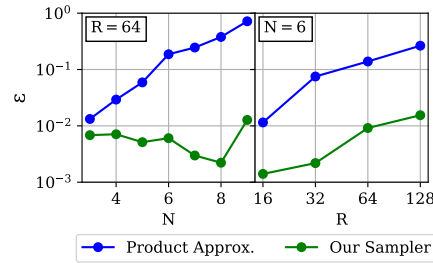


Figure 3. ε for varying R and N on least-squares solves, $I = 2^{16}$, $J = 5000$. Datapoints are averages of 50 measurements.

when the full Khatri-Rao product has $\approx 3.78 \times 10^{22}$ rows (for $I = 2^{25}$, $N = 3$, $R = 32$), we require only 0.31 seconds on average for sampling.

4.2. Least-Squares Accuracy Comparison

We now test our sampler on least-squares problems of the form $\min_x \|Ax - b\|$, where $A = U_1 \odot \dots \odot U_N$ with $U_j \in \mathbb{R}^{I \times R}$ for all j . We initialize all matrices U_j entrywise i.i.d. from a standard normal distribution and randomly multiply 1% of all entries by 10. We choose b as a Kronecker product $c_1 \otimes \dots \otimes c_N$, with each vector $c_j \in \mathbb{R}^I$ also initialized entrywise from a Gaussian distribution.

Define $\varepsilon = \frac{\text{residual}_{\text{approx}}}{\text{residual}_{\text{opt}}} - 1$, where $\text{residual}_{\text{approx}}$ is the residual of a randomized least-squares algorithm. ε is always positive and (similar to its role in theorem 2.1) quantifies the quality of the randomized algorithm’s solution. For varying N and R , figure 3 shows the values ε achieved by our algorithm against the leverage product approximation used by Cheng et al. and Larsen and Kolda (2016; 2022). Our sampler achieves $\varepsilon \approx 10^{-2}$ even when $N = 9$, while the product approximation increases its error by nearly two orders of magnitude.

Fast Exact Leverage Score Sampling from Khatri-Rao Products

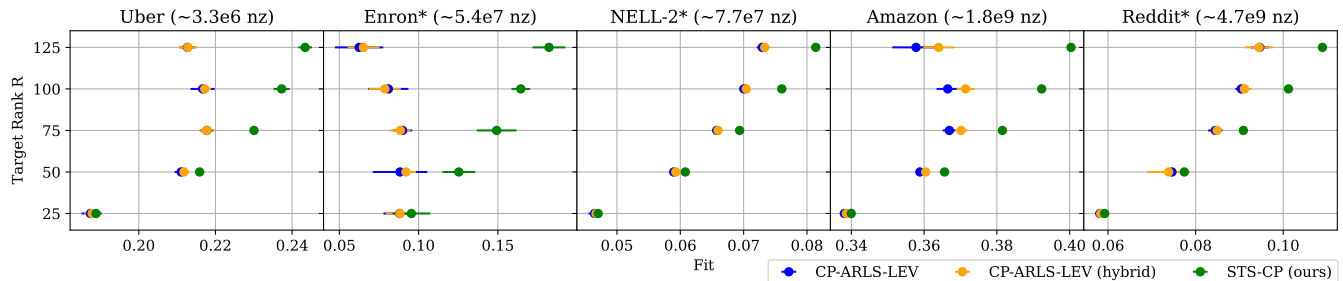


Figure 4. Fit achieved by randomized ALS algorithms for sparse tensor CP decomposition. All methods draw $J = 2^{16}$ samples per least-squares solve. Each datapoint is an average of 8 trials and error bars indicate 3 standard deviations. See A.7 for details.

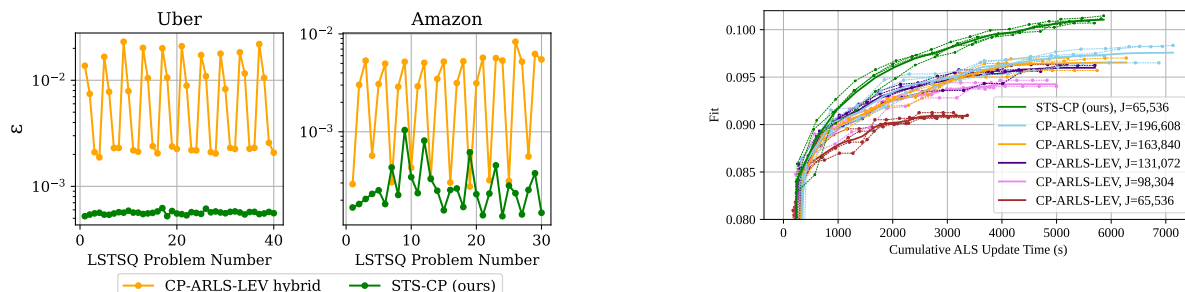


Figure 5. Value of ε for randomized least squares solves in the first 10 rounds of ALS on sparse tensors, $R = 50$. Datapoints are averages across 5 ALS runs with the same initial factors.

4.3. Sparse Tensor Decomposition

We next apply STS-CP to decompose several large sparse tensors from the FROSTT collection (Smith et al., 2017) (see appendix A.7 for more details on the experimental configuration). Our accuracy metric is the tensor fit. Letting $\tilde{\mathcal{T}}$ be our low-rank CP approximation, the fit with respect to ground-truth tensor \mathcal{T} is $\text{fit}(\tilde{\mathcal{T}}, \mathcal{T}) = 1 - \frac{\|\tilde{\mathcal{T}} - \mathcal{T}\|_F}{\|\mathcal{T}\|_F}$. The best possible fit achievable through low-rank CP decomposition varies significantly from tensor to tensor. Even with a fit as low as ≈ 0.06 achieved by exact ALS on the Reddit tensor ($R = 25$), Larsen and Kolda recover useful signals from the factor matrices (2022).

As figure 4 shows, the fit achieved by CP-ARLS-LEV compared to STS-CP degrades as the rank increases for fixed sample count. By contrast, STS-CP improves the fit consistently, with a significant improvement at rank 125 over CP-ARLS-LEV. Figure 5 explains the higher fit achieved by our sampler on the Uber and Amazon tensors. In the first 10 rounds of ALS, we compute the exact solution to each least-squares problem before updating the factor matrix with a randomized algorithm’s solution. Figure 5 plots ε as ALS progresses for hybrid CP-ARLS-LEV and STS-CP. The latter achieves lower residual per solve. We further note that CP-ARLS-LEV exhibits an oscillating error pattern based on the tensor mode isolated in each ALS update.

To assess the tradeoff between sampling time and accuracy,

Figure 6. Fit as a function of ALS update time, Reddit tensor, $R = 100$. Thick lines average the interpolations of running max fits across 4 runs (thin dotted lines).

we compare the fit as a function of ALS update time for STS-CP and random CP-ARLS-LEV in figure 6 (time to compute the fit excluded). On the Reddit tensor with $R = 100$, we compared CP-ARLS-LEV with $J = 2^{16}$ against CP-ARLS-LEV with progressively increasing sample count. Even with 2^{18} samples per randomized least-squares solve, CP-ARLS-LEV cannot achieve the maximum fit of STS-CP. Furthermore, STS-CP makes progress more quickly than CP-ARLS-LEV. See appendix A.8.3 for similar plots.

5. Discussion and Future Work

Our method for exact Khatri-Rao leverage score sampling enjoys strong theoretical guarantees and practical performance benefits. On the Enron tensor, STS-CP achieves an average fit 2.8 times larger than CP-ARLS-LEV for $J = 2^{16}$, $R = 125$, demonstrating that our algorithm’s superior sample efficiency translates to significant accuracy gain. Especially for massive tensors such as Amazon and Reddit, our randomized algorithm makes faster progress and achieves a higher final fit.

The segment tree approach described here can be applied to sample from tensor networks besides the Khatri-Rao product. In particular, modifications to lemma 3.2 permit efficient leverage sampling from a contraction of 3D tensor cores in ALS tensor train decomposition. We leave the generalization of our fast sampling technique as future work.

References

- Ailon, N. and Chazelle, B. The fast johnson–lindenstrauss transform and approximate nearest neighbors. *SIAM Journal on computing*, 39(1):302–322, 2009.
- Cheng, D., Peng, R., Liu, Y., and Perros, I. SPALS: Fast Alternating Least Squares via Implicit Leverage Scores Sampling. In *Advances in Neural Information Processing Systems*, volume 29. Curran Associates, Inc., 2016.
- Derezinski, M. and Mahoney, M. W. Determinantal point processes in randomized numerical linear algebra. *Notices of the American Mathematical Society*, 68(1):34–45, 2021.
- Drineas, P., Magdon-Ismail, M., Mahoney, M. W., and Woodruff, D. P. Fast approximation of matrix coherence and statistical leverage. *J. Mach. Learn. Res.*, 13(1): 3475–3506, dec 2012. ISSN 1532-4435.
- Haidar, A., Dong, T., Tomov, S., Luszczek, P., and Dongarra, J. Framework for batched and gpu-resident factorization algorithms to block householder transformations. In *ISC High Performance*, Frankfurt, Germany, 07-2015 2015. Springer, Springer.
- Halko, N., Martinsson, P. G., and Tropp, J. A. Finding structure with randomness: Probabilistic algorithms for constructing approximate matrix decompositions. *SIAM Review*, 53(2):217–288, 2011. doi: 10.1137/090771806.
- Jin, R., Kolda, T. G., and Ward, R. Faster Johnson–Lindenstrauss transforms via Kronecker products. *Information and Inference: A Journal of the IMA*, 10(4):1533–1562, October 2020. ISSN 2049-8772. doi: 10.1093/imaiai/iaaa028. _eprint: <https://academic.oup.com/imaiai/article-pdf/10/4/1533/41748789/iaaa028.pdf>.
- Kolda, T. G. and Bader, B. W. Tensor Decompositions and Applications. *SIAM Review*, 51(3):455–500, August 2009. ISSN 0036-1445. doi: 10.1137/07070111X. URL <https://epubs.siam.org/doi/10.1137/07070111X>. Publisher: Society for Industrial and Applied Mathematics.
- Larsen, B. W. and Kolda, T. G. Practical Leverage-Based Sampling for Low-Rank Tensor Decomposition. *SIAM J. Matrix Analysis and Applications*, 43(3):1488–1517, August 2022. doi: 10.1137/21M1441754. _eprint: 2006.16438.
- Ma, L. and Solomonik, E. Cost-efficient gaussian tensor network embeddings for tensor-structured inputs. *CoRR*, abs/2205.13163, 2022. doi: 10.48550/arXiv.2205.13163. URL <https://doi.org/10.48550/arXiv.2205.13163>.
- Malik, O. A. More efficient sampling for tensor decomposition with worst-case guarantees. In Chaudhuri, K., Jegelka, S., Song, L., Szepesvari, C., Niu, G., and Sabato, S. (eds.), *Proceedings of the 39th International Conference on Machine Learning*, volume 162 of *Proceedings of Machine Learning Research*, pp. 14887–14917. PMLR, 17–23 Jul 2022. URL <https://proceedings.mlr.press/v162/malik22a.html>.
- Malik, O. A., Bharadwaj, V., and Murray, R. Sampling-Based Decomposition Algorithms for Arbitrary Tensor Networks, October 2022. URL <http://arxiv.org/abs/2210.03828>. arXiv:2210.03828 [cs, math].
- Martens, J. and Grosse, R. Optimizing neural networks with Kronecker-factored approximate curvature. In *Proceedings of the 32nd International Conference on International Conference on Machine Learning - Volume 37*, ICML’15, pp. 2408–2417, Lille, France, July 2015. JMLR.org.
- Saad, F. A., Freer, C. E., Rinard, M. C., and Mansinghka, V. K. Optimal Approximate Sampling from Discrete Probability Distributions. *Proceedings of the ACM on Programming Languages*, 4(POPL):1–31, January 2020. ISSN 2475-1421. doi: 10.1145/3371104. URL <http://arxiv.org/abs/2001.04555>. arXiv:2001.04555 [cs, math, stat].
- Smith, S., Choi, J. W., Li, J., Vuduc, R., Park, J., Liu, X., and Karypis, G. FROSTT: The formidable repository of open sparse tensors and tools, 2017. URL <http://frostdt.io/>.
- Walker, A. New fast method for generating discrete random numbers with arbitrary frequency distributions. *Electronics Letters*, 10:127–128(1), April 1974. ISSN 0013-5194.
- Wang, Y., Tung, H.-Y., Smola, A. J., and Anandkumar, A. Fast and guaranteed tensor decomposition via sketching. *Advances in neural information processing systems*, 28, 2015.
- Woodruff, D. P. et al. Sketching as a tool for numerical linear algebra. *Foundations and Trends® in Theoretical Computer Science*, 10(1–2):1–157, 2014.

A. Appendix

A.1. Details about Table 1

CP-ALS is the standard alternating least-squares algorithm that performs the update in equation (14) using non-randomized least-squares (Kolda & Bader, 2009). CP-ARLS-LEV is the algorithm proposed by Larsen and Kolda (2022) that samples rows from the Khatri-Rao product according to a product distribution of leverage scores on each factor matrix. The per-iteration runtimes for both algorithms are re-derived in appendix C.3 of the work by Malik (2022) from their original sources. Malik proposed the CP-ALS-ES algorithm (not listed in the table), which is superseded by the TNS-CP algorithm (Malik et al., 2022). We report the complexity from table 1 of the latter work. The algorithm from Ma and Solomonik (2022) is based on a general method to sketch tensor networks. Our reported complexity is listed in table 1 for algorithm 1 in their work.

Table 1 does not list the one-time initialization costs for any of the methods. All methods require at least $O(NIR)$ time to randomly initialize factor matrices, and CP-ALS requires no further setup. CP-ARLS-LEV, TNS-CP, and STS-CP all require $O(NIR^2)$ initialization time. CP-ARLS-LEV uses the initialization phase to compute the initial leverage scores of all factor matrices. TNS-CP uses the initialization step to compute and cache gram matrices of all factors U_j . STS-CP must build the efficient sampling data structure described in 1.1. The algorithm from Ma and Solomonik requires an initialization cost of $O(I^N m)$, where m a sketch size parameter that is $O(NR/\varepsilon^2)$ to achieve the (ε, δ) accuracy guarantee for each least-squares solve.

A.2. Proof of Lemma 3.2

By exhibit. We detail the construction procedure, sampling procedure, and correctness of our proposed data structure.

Construction: Algorithm 4 gives the procedure to build the data structure. We initialize a segment tree $T_{I,F}$ and compute G^v for all leaf nodes $v \in T_{I,F}$ as a sum of outer products of rows from U (lines 1-3). Starting at the level above the leaves, we then compute G^v for each internal node as the sum of $G^{L(v)}$ and $G^{R(v)}$, the partial gram matrices of its two children. Runtime $O(IR^2)$ is required to compute I outer products across all iterations of the loop on line 3. Our segment tree has $\lceil I/F \rceil - 1$ internal nodes, and the addition in line 6 contributes runtime $O(R^2)$ for each internal node. This adds complexity $O(R^2(\lceil I/F \rceil - 1)) \leq O(IR^2)$, for total construction time $O(IR^2)$. To analyze the space complexity, observe that we store a matrix $G^v \in \mathbb{R}^{R \times R}$ at all $2\lceil I/F \rceil - 1$ nodes of the segment tree, for asymptotic space usage $O(\lceil I/F \rceil R^2)$. We can cut the space usage in half by only storing G^v when v is either the root or a left child in our tree, since algorithm 1 only executes \tilde{m} on nodes v that are left children. We can cut the space usage in half again by only storing the upper triangle of each symmetric matrix G^v . Finally, in the special case that $I < F$, the segment tree has depth 1 and no calls to \tilde{m} are needed. As a result, the data structure has $O(1)$ space overhead because we can avoid storing any partial gram matrices G^v .

Algorithm 4 BuildSampler($U \in \mathbb{R}^{I \times R}$, F , Y)

- 1: Build tree $T_{I,F}$ with depth $d = \lceil \log \lceil I/F \rceil \rceil$
 - 2: **for** $v \in \text{leaves}(T_{I,F})$ **do**
 - 3: $G^v := \sum_{i \in S(v)} U[i, :]^\top U[i, :]$
 - 4: **for** $u = d - 2 \dots 0$ **do**
 - 5: **for** $v \in \text{level}(T_{I,F}, u)$ **do**
 - 6: $G^v := G^{L(v)} + G^{R(v)}$
-

Sampling: Algorithm 5 gives the procedure to draw a sample from our proposed data structure. It is easy to verify that the normalization constant C for $q_{h,U,Y}$ is $\langle hh^\top, G^{\text{root}(T_{I,F})}, Y \rangle$, since $G^{\text{root}(T_{I,F})} = U^\top U$. If $C = 0$, we return an index from I uniformly at random. Otherwise, we initialize procedures \tilde{m} and \tilde{q} and pass their partial evaluations to the STSample procedure. Each execution of procedure \tilde{m} requires time $O(R^2)$, relying on the partial gram matrices G^v computed during the construction phase. When Y is a general p.s.d. matrix, the runtime of \tilde{q} is $O(FR^2)$. This complexity is dominated by the matrix multiplication $W \cdot (hh^\top \otimes Y)$ on line 5. By equation (2) with $\tau_1 = O(R^2)$ and $\tau_2(F) = O(FR^2)$, the runtime to draw one sample is $O(R^2 \log \lceil I/F \rceil + FR^2)$. When $Y = [1]$, we have $hh^\top \otimes Y = hh^\top$. This gives

$$\tilde{q}_p(h, C, v) = \text{diag}(W \cdot (hh^\top) \cdot W) = (W \cdot h)^2$$

where the square is elementwise. The runtime $\tau_2(F)$ of procedure \tilde{q} is now dominated by a matrix-vector multiplication that costs time $O(FR)$. In this case, we have per-sample complexity $O(R^2 \log \lceil I/F \rceil + FR)$.

Algorithm 5 Row Sampling Procedure

Require: Matrices U, Y saved from construction, partial gram matrices $\{G^v \mid v \in T_{I,F}\}$.

- 1: **procedure** $\tilde{m}_p(h, C, v)$
 - 2: **return** $C^{-1} \langle hh^\top, G^v, Y \rangle$
 - 3: **procedure** $\tilde{q}_p(h, C, v)$
 - 4: $W := U[S(v), :]$
 - 5: **return** $C^{-1} \text{diag}(W \cdot (hh^\top \otimes Y) \cdot W^\top)$
 - 6: **procedure** RowSample(h)
 - 7: $C := \langle hh^\top, G^{\text{root}(T_{I,F})}, Y \rangle$
 - 8: $\tilde{m}(\cdot) := \tilde{m}_p(h, C, \cdot)$
 - 9: $\tilde{q}(\cdot) := \tilde{q}_p(h, C, \cdot)$
 - 10: **return** STSample($T_{I,F}, \tilde{m}(\cdot), \tilde{q}(\cdot)$)
-

Correctness: The construction procedure correctly initializes the partial gram matrices G^v for all $v \in T_{I,F}$. Equations (4) and (6) show that the functions $\tilde{m}(\cdot)$ and $\tilde{q}(\cdot)$ satisfy the conditions of proposition 3.1. Hence, the STSample procedure correctly returns a row index according to the distribution $q_{h,U,Y}$. \square

A.3. Proof of Theorem 3.3

Theorem 3.3 first appeared in a modified form as lemma 10 in the work by Malik (2022). This original version used the definition $\tilde{G}_{>k} = \Phi \circledast \bigcircledast_{a=k+1}^N G_k$ in place of $G_{>k}$ defined in equation (9), where Φ was a sketched approximation of G^+ . We prove the modified version stated in our work instead.

Proof of Theorem 3.3. We rely on the assumption that the Khatri-Rao product A is a nonzero matrix (but it may be rank-deficient). Beginning with equation (7), we derive

$$\begin{aligned}
 \ell_{i_1, \dots, i_N} &= A[(i_1, \dots, i_N), :] G^+ A[(i_1, \dots, i_N), :]^\top \\
 &= \langle A[(i_1, \dots, i_N), :]^\top A[(i_1, \dots, i_N), :], G^+ \rangle \\
 &= \left\langle \left(\bigcircledast_{a=1}^N U_a[i_a, :] \right)^\top \left(\bigcircledast_{a=1}^N U_a[i_a, :] \right), G^+ \right\rangle \\
 &= \left\langle \bigcircledast_{a=1}^N U_a[i_a, :]^\top U_a[i_a, :], G^+ \right\rangle \\
 &= \left\langle \bigcircledast_{a=1}^{k-1} U_a[i_a, :]^\top U_a[i_a, :], U_k[i_k, :]^\top U_k[i_k, :] \circledast \bigcircledast_{a=k+1}^N U_a[i_a, :]^\top U_a[i_a, :], G^+ \right\rangle \\
 &= \left\langle \bigcircledast_{a=1}^{k-1} U_a[i_a, :]^\top U_a[i_a, :], U_k[i_k, :]^\top U_k[i_k, :], G^+ \circledast \bigcircledast_{a=k+1}^N U_a[i_a, :]^\top U_a[i_a, :] \right\rangle.
 \end{aligned} \tag{15}$$

To compute $p(\hat{s}_k = s_k \mid \hat{s}_{<k} = s_{<k})$, we marginalize over random variables $\hat{s}_{k+1} \dots \hat{s}_N$. Recalling the definition of $h_{<k}$ from equation (8), we have

$$\begin{aligned}
 &p(\hat{s}_k = s_k \mid \hat{s}_{<k} = s_{<k}) \\
 &\propto \sum_{i_{k+1}, \dots, i_N} p\left(\hat{s}_{<k} = s_{<k} \wedge (\hat{s}_k = s_k) \wedge \bigwedge_{u=1}^N \hat{s}_u = i_u\right) \\
 &= \sum_{i_{k+1}, \dots, i_N} \ell_{s_1, \dots, s_k, i_{k+1}, \dots, i_N} \\
 &= \sum_{i_{k+1}, \dots, i_N} \left\langle \bigcircledast_{a=1}^{k-1} U_a[s_a, :]^\top U_a[s_a, :], U_k[s_k, :]^\top U_k[s_k, :], G^+ \circledast \bigcircledast_{a=k+1}^N U_a[i_a, :]^\top U_a[i_a, :] \right\rangle \\
 &= \sum_{i_{k+1}, \dots, i_N} \langle h_{<k} h_{<k}^\top, U_k[s_k, :]^\top U_k[s_k, :], G^+ \circledast \bigcircledast_{a=k+1}^N U_a[i_a, :]^\top U_a[i_a, :] \rangle \\
 &= \langle h_{<k} h_{<k}^\top, U_k[s_k, :]^\top U_k[s_k, :], G^+ \circledast \bigcircledast_{a=k+1}^N \sum_{i_a=1}^{|I_a|} U_a[i_a, :]^\top U_a[i_a, :] \rangle \\
 &= \langle h_{<k} h_{<k}^\top, U_k[s_k, :]^\top U_k[s_k, :], G^+ \circledast \bigcircledast_{a=k+1}^N G_a \rangle \\
 &= \langle h_{<k} h_{<k}^\top, U_k[s_k, :]^\top U_k[s_k, :], G_{>k} \rangle.
 \end{aligned} \tag{16}$$

We now compute the normalization constant C for the distribution by summing equation 16 over all possible values for \hat{s}_k :

$$\begin{aligned}
 C &= \sum_{s_k=1}^{|I_k|} \langle h_{<k} h_{<k}^\top, U_k [s_k, :]^\top U_k [s_k, :], G_{>k} \rangle \\
 &= \langle h_{<k} h_{<k}^\top, \sum_{s_k=1}^{|I_k|} U_k [s_k, :]^\top U_k [s_k, :], G_{>k} \rangle \\
 &= \langle h_{<k} h_{<k}^\top, G_k, G_{>k} \rangle.
 \end{aligned} \tag{17}$$

This matches the claim. For $k = 1$, we have $h_{<k} = [1, \dots, 1]^\top$, so $C = \langle G_k, G_{>k} \rangle$. Then C is the sum of all leverage scores, which is known to be the rank of A (Woodruff et al., 2014). Since A was assumed nonzero, $C \neq 0$. For $k > 1$, assume that the conditioning event $\hat{s}_{<k} = s_{<k}$ occurs with nonzero probability. This implies

$$\begin{aligned}
 p(\hat{s}_{k-1} = s_{k-1} \mid \hat{s}_{<k-1} = s_{<k-1}) &= \langle h_{<k-1} h_{<k-1}^\top, U_{k-1} [s_{k-1}, :]^\top U_{k-1} [s_{k-1}, :], G_{>k-1} \rangle \\
 &= \langle h_{<k} h_{<k}^\top, G_{>k-1} \rangle \\
 &= \langle h_{<k} h_{<k}^\top, G_k \otimes G_{>k} \rangle \\
 &= \langle h_{<k} h_{<k}^\top, G_k, G_{>k} \rangle \\
 &> 0,
 \end{aligned} \tag{18}$$

so C is nonzero in this case as well. \square

A.4. Cohesive Proof of Theorem 1.1

In this proof, we fully explain algorithms 2 and 3 in the context of the sampling procedure outlined in section 3.3. We verify the complexity claims first and then prove correctness.

Construction and Update: For each matrix U_j , algorithm 2 builds an efficient row sampling data structure Z_j as specified by lemma 3.2. We let the p.s.d. matrix Y that parameterizes each sampler be a matrix of ones, and we set $F = R$. From lemma 3.2, the time to construct sampler Z_j is $O(|I_j| R^2)$. The space used by sampler Z_j is $O(\lceil |I_j| / F \rceil R^2) = O(|I_j| R)$, since $F = R$. In case $|I_j| < R$, we use the special case described in A.2 to get a space overhead $O(1)$, avoiding a term $O(R^2)$ in the space complexity.

Summing the time and space complexities over all j proves part 1 of the theorem. To update the data structure if matrix U_j changes, we only need to rebuild sampler Z_j for a cost of $O(|I_j| R^2)$. The construction phase also computes and stores the gram matrix G_j for each matrix U_j .

Sampling: For all indices k (except possibly j), lines 1-5 from algorithm 3 compute $G_{>k}$ and its eigendecomposition. Only a single pass over the gram matrices G_k is needed, so these steps cost $O(R^3)$ for each index k . Line 5 builds an efficient row sampler E_k for the matrix of scaled eigenvectors $\sqrt{\Lambda_k} \cdot V_k$. For sampler k , we set $Y = G_k$ with cutoff parameter $F = 1$. From lemma 3.2, the construction cost is $O(R^3)$ for each index k , and the space required by each sampler is $O(R^3)$. Summing these quantities over all $k \neq j$ gives asymptotic runtime $O(NR^3)$ and scratch space usage $O(NR^3)$ for lines 2-5.

The loop spanning lines 6-12 draws J row indices from the Khatri-Rao product $U_{\neq j}$. For each sample, we maintain a ‘‘history vector’’ h to write the variables $h_{<k}$ from equation (8). For each index $k \neq j$, we draw random variable \hat{u}_k using the row sampler E_k . This random draw indexes a scaled eigenvector of $G_{>k}$. We then use the history vector h multiplied by the eigenvector to sample a row index \hat{t}_k using data structure Z_k . The history vector h is updated, and we proceed to draw the next index \hat{t}_k .

From lemma 3.2, lines 9 and 10 cost $O(R^2 \log R)$ and $O(R^2 \log \lceil |I_k| / R \rceil)$, respectively. Line 11 costs $O(R)$ and contributes a lower-order term. Summing over all $k \neq j$, the runtime to draw a single sample is

$$O \left(\sum_{k \neq j} (R^2 \log \lceil |I_k| / R \rceil + R^2 \log R) \right) = O \left(\sum_{k \neq j} R^2 \log \max(|I_k|, R) \right).$$

Adding the runtime for all J samples to the runtime of the loop spanning lines 2-6 gives runtime $O(NR^3 + J \sum_{k \neq j} R^2 \log \max(|I_k|, R))$, and the complexity claims have been proven.

Correctness: We show correctness for the case where $j = -1$ and we sample from the Khatri-Rao product of all matrices U_k , since the proof for any other value of j requires a simple reindexing of matrices. To show that our sampler is correct, it is enough to prove the condition that for $1 \leq k \leq N$,

$$p(\hat{t}_k = t_k \mid h_{<k}) = q_{h_{<k}, U_k, G_{>k}}[t_k], \quad (19)$$

since, by theorem 3.3, $p(\hat{s}_k = s_k \mid \hat{s}_{<k} = s_{<k}) = q_{h_{<k}, U_k, G_{>k}}[s_k]$. This would imply that the joint random variable $(\hat{t}_1, \dots, \hat{t}_N)$ has the same probability distribution as $(\hat{s}_1, \dots, \hat{s}_N)$, which by definition follows the leverage score distribution on $U_1 \odot \dots \odot U_N$. To prove the condition in equation (19), we just apply equations (12) and (13) derived earlier:

$$\begin{aligned} p(\hat{t}_k = t_k \mid h_k) &= \sum_{u_k=1}^R p(\hat{t}_k = t_k \mid \hat{u}_k = u_k, h_{<k}) p(\hat{u}_k = u_k \mid h_{<k}) && \text{(Bayes' Rule)} \\ &= \sum_{u_k=1}^R e[u_k] \frac{W[t_k, u_k]}{\|W[:, u_k]\|_1} && \text{(Equations (12) and (13), in reverse)} \\ &= q_{h_{<k}, U_k, G_{>k}}[t_k]. \end{aligned} \quad (20)$$

□

A.5. Alternating Least Squares CP Decomposition

Let U_1, \dots, U_N be factor matrices of a low-rank CP decomposition, $U_k \in \mathbb{R}^{|I_k| \times R}$. By $U_{\neq j}$, we denote the Khatri-Rao product of all matrices U_k except U_j . The matricization $\text{mat}(\mathcal{T}, j)$ flattens tensor \mathcal{T} into a matrix and isolates mode j . The output of matricization is a $\prod_{k \neq j} |I_k| \times |I_j|$ matrix, with each row containing a mode- j fiber from \mathcal{T} . Below, we prove corollary 3.4.

Proof of Corollary 3.4. The design matrix for optimization problem j within a round of ALS has dimensions $\prod_{k \neq j} |I_k| \times R$, and the observation matrix has dimensions $\prod_{k \neq j} |I_k| \times |I_j|$. To achieve error threshold $1 + \varepsilon$ with probability $1 - \delta$ on each solve, we draw $J = O(R/(\varepsilon\delta))$ rows from both the design and observation matrices and solve the downsampled problem (theorem 2.1). These rows are sampled according to the leverage score distribution on the rows of $U_{\neq j}$, for which we use the data structure in theorem 1.1. After a one-time initialization cost $O(\sum_{j=1}^N |I_j| R^2)$ before the ALS iteration begins, the complexity to draw J samples (assuming $|I_j| \geq R$) is

$$O\left(NR^3 + J \sum_{k \neq j} R^2 \log |I_k|\right) = O\left(NR^3 + \frac{R}{\varepsilon\delta} \sum_{k \neq j} R^2 \log |I_k|\right).$$

The cost to assemble the corresponding subset of the observation matrix is $O(J |I_j|) = O(R |I_j| / (\varepsilon\delta))$. The cost to solve the downsampled least-squares problem is $O(JR^2) = O(|I_j| R^2 / (\varepsilon\delta))$, which dominates the cost of forming the subset of the observation matrix. Finally, we require additional time $O(|I_j| R^2)$ to update the sampling data structure (theorem 1.1 part 1). Adding these terms together and summing over $1 \leq j \leq N$ gives

$$\begin{aligned} &O\left(\frac{1}{\varepsilon\delta} \cdot \sum_{j=1}^N \left[|I_j| R^2 + \sum_{k \neq j} R^3 \log |I_k| \right]\right) \\ &= O\left(\frac{1}{\varepsilon\delta} \cdot \sum_{j=1}^N [|I_j| R^2 + (N-1)R^3 \log |I_j|]\right). \end{aligned} \quad (21)$$

Rounding $N-1$ to N and multiplying by the number of iterations gives the desired complexity. When $|I_j| < R$ for any j , the complexity changes in theorem 1.1 propagate to the equation above. □

In practice, ALS iteration is stabilized by renormalizing the factor matrix columns to unit norm after each least-squares solve. These column norms are collected in a coefficient vector $\sigma_1, \dots, \sigma_R$, which are analogous to the singular values in the matrix SVD. Column normalization costs additional time $O(\sum_{j=1}^N |I_j| R)$ per round of ALS, a lower-order term. We perform column renormalization in our ALS implementation.

A.6. Experimental Platform and Sampler Parallelism

We provide two implementations of our sampler. The first is a slow reference implementation written entirely in Python, which closely mimics our pseudocode and can be used to test correctness. The second is an efficient implementation written in C++, parallelized in shared memory with OpenMP and Intel Thread Building Blocks.

Each Perlmutter CPU node (our experimental platform) is equipped with two sockets, each containing an AMD EPYC 7763 processor with 64 cores. All benchmarks were conducted with our efficient C++ implementation using 128 OpenMP threads. We linked our code against Intel Thread Building blocks to call a multithreaded sort function when decomposing sparse tensors. We use OpenBLAS 0.3.21 to handle linear algebra with OpenMP parallelism enabled, but our code links against any linear algebra library implementing the CBLAS and LAPACKE interfaces.

Our proposed data structure samples from the exact distribution of leverage scores of the Khatri-Rao product, thereby enjoying better sample efficiency than alternative approaches such as CP-ARLS-LEV (Larsen & Kolda, 2022). The cost to draw each sample, however, is $O(R^2 \log H)$, where H is the number of rows in the Khatri-Rao product. Methods such as row-norm-squared sampling or CP-ARLS-LEV can draw each sample in time $O(\log H)$ after appropriate preprocessing. Therefore, efficient parallelization of our sampling procedure is required for competitive performance, and we present two strategies below.

1. **Asynchronous Thread Parallelism:** The KRPSampleDraw procedure in algorithm 3 can be called by multiple threads concurrently without data races. The simplest parallelization strategy divides the J samples equally among the threads in a team, each of which makes calls to KRPSampleDraw asynchronously. This strategy works well on a CPU, but is less attractive on a SIMT processor like a GPU where instruction streams cannot diverge without significant performance penalties.
2. **Synchronous Batch Parallelism** As an alternative to the asynchronous strategy, suppose for the moment that all leaves have the same depth in each segment tree. Then for every sample, STSample makes an sequence of calls to \tilde{m} , each updating the current node by branching left or right in the tree. The length of this sequence is the depth of the tree, and it is followed by a single call to the function \tilde{q} . Observe that the right-hand side of equation (4) can be computed with a matrix-vector multiplication followed by a dot product. The right-hand side of equation (5) requires the same two operations if $F = 1$ or $Y = [1]$. Thus, we can create a batched version of the STSample procedure that makes a fixed length sequence of calls to batched `gemv` and `dot` routines. All processors march in lock-step down the levels of the segment tree, each of them tracking the branching path of a single sample. The MAGMA linear algebra library provides a batched version of `gemv` (Haidar et al., 2015), while a batched dot product can be implemented with an ad hoc kernel. MAGMA also offers a batched version of the symmetric rank- k update routine `syrk`, which is helpful to parallelize row sampler construction (algorithm 4). When all leaves in the tree are not at the same level, the the bottom level of the tree can be handled with a special sequence of instructions making the required additional calls to \tilde{m} .

Our CPU code follows the batch synchronous design pattern. To avoid dependency on GPU-based MAGMA routines in our CPU prototype, however, portions of the code that should be batched BLAS calls are standard BLAS calls wrapped in a `for` loop. These sections can be easily replaced when the appropriate batched routines are available.

A.7. Sparse Tensor CP Experimental Configuration

Table 2. Sparse Tensors from FROSTT collection.

TENSOR	DIMENSIONS	NONZEROS	PREPROCESSING	INITIALIZATION
UBER PICKUPS	$183 \times 24 \times 1,140 \times 1,717$	3,309,490	NONE	IID
ENRON EMAILS	$6,066 \times 5,699 \times 244,268 \times 1,176$	54,202,099	LOG VALUES	RRF
NELL-2	$12,092 \times 9,184 \times 28,818$	76,879,419	LOG VALUES	IID
AMAZON REVIEWS	$4,821,207 \times 1,774,269 \times 1,805,187$	1,741,809,018	NONE	IID
REDDIT-2015	$8,211,298 \times 176,962 \times 8,116,559$	4,687,474,081	LOG VALUES	IID

Table 2 lists the nonzero counts and dimensions of sparse tensors in our experiments (Smith et al., 2017). We took the log of all values in the Enron, NELL-2, and Reddit-2015 tensors. Consistent with established practice, this operation damps the effect of a few high magnitude tensor entries on the fit metric (Larsen & Kolda, 2022).

The factor matrices for the Uber, Amazon, NELL-2, and Reddit experiments were initialized with i.i.d. entries from the standard normal distribution. As suggested by Larsen and Kolda, the Enron tensor’s factors were initialized with a randomized range finder (2022; 2011). This algorithm initializes each factor matrix as a random linear combination of fibers along each tensor mode. Larsen and Kolda used a subset of the fibers along each mode, while we ran a “complete” randomized range finder with all fibers.

ALS was run for a maximum of 40 rounds on all tensors except for Reddit, which was run for 80 rounds. The exact fit was computed every 5 rounds (defined as 1 epoch), and we used an early stopping condition to terminate runs early. The algorithm was terminated at iteration T if the maximum fit in the last 3 epochs did not exceed the maximum fit from epoch 1 through epoch $T - 3$ by tolerance 10^{-4} .

Hybrid CP-ARLS-LEV deterministically includes rows from the Khatri-Rao product whose probabilities exceed a threshold τ . The ostensible goal of this procedure is to improve diversity in sample selection, as CP-ARLS-LEV may suffer from many repeat draws of high probability rows. We replicate the conditions proposed in the original work by selecting $\tau = 1/J$ (Larsen & Kolda, 2022).

A.8. Supplementary Results

A.8.1. PROBABILITY DISTRIBUTION COMPARISON

Figure 7 provides confirmation on a small test problem that our sampler works as expected. For the Khatri-Rao product of three matrices $A = U_1 \odot U_2 \odot U_3$, it plots the true distribution of leverage scores against a normalized histogram of 50,000 draws from the data structure in theorem 1.1. We choose $U_1, U_2, U_3 \in \mathbb{R}^{8 \times 8}$ initialized i.i.d. from a standard normal distribution with 1% of all entries multiplied by 10. We observe excellent agreement between the histogram and the true distribution.

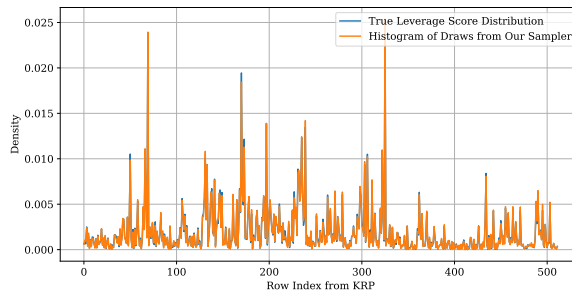


Figure 7. Comparison of true leverage score distribution with histogram of 50,000 samples drawn from $U_1 \odot U_2 \odot U_3$.

A.8.2. FITS ACHIEVED FOR $J = 2^{16}$

Table 3 gives the fits achieved for sparse tensor decomposition for varying rank and algorithm (presented graphically in figure 4). Uncertainties are one standard deviation across 8 runs of ALS.

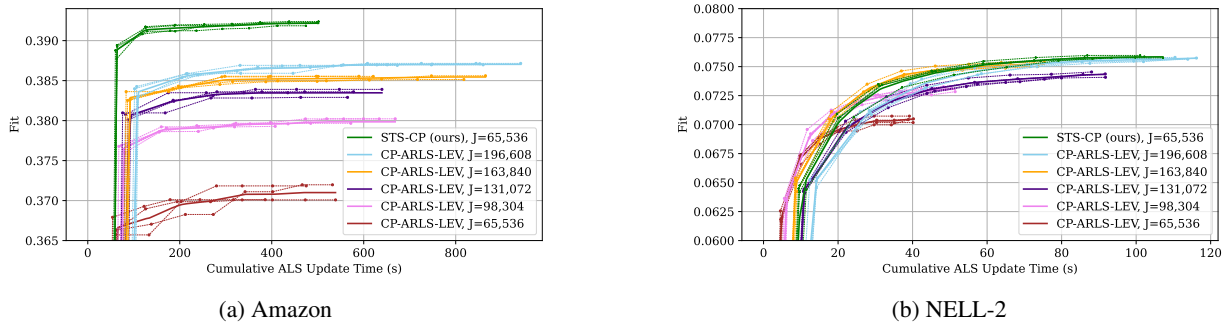


Figure 8. Fit as a function of time, $R = 100$.

Table 3. Fits Achieved for Sparse Tensor Decomposition, $J = 2^{16}$.

TENSOR	RANK	CP-ARLS-LEV (RAND)	CP-ARLS-LEV (HYBRID)	STS-CP (OURS)
UBER	25	$0.187 \pm 2.30E-03$	$0.188 \pm 2.11E-03$	$0.189 \pm 1.52E-03$
	50	$0.211 \pm 1.72E-03$	$0.212 \pm 1.27E-03$	$0.216 \pm 1.18E-03$
	75	$0.218 \pm 1.76E-03$	$0.218 \pm 2.05E-03$	$0.230 \pm 9.24E-04$
	100	$0.217 \pm 3.15E-03$	$0.217 \pm 1.69E-03$	$0.237 \pm 2.12E-03$
	125	$0.213 \pm 1.96E-03$	$0.213 \pm 2.47E-03$	$0.243 \pm 1.78E-03$
ENRON	25	$0.0881 \pm 1.02E-02$	$0.0882 \pm 9.01E-03$	$0.0955 \pm 1.19E-02$
	50	$0.0883 \pm 1.72E-02$	$0.0920 \pm 6.32E-03$	$0.125 \pm 1.03E-02$
	75	$0.0899 \pm 6.10E-03$	$0.0885 \pm 6.39E-03$	$0.149 \pm 1.25E-02$
	100	$0.0809 \pm 1.26E-02$	$0.0787 \pm 1.00E-02$	$0.164 \pm 5.90E-03$
	125	$0.0625 \pm 1.52E-02$	$0.0652 \pm 1.00E-02$	$0.182 \pm 1.04E-02$
NELL-2	25	$0.0465 \pm 9.52E-04$	$0.0467 \pm 4.61E-04$	$0.0470 \pm 4.69E-04$
	50	$0.0590 \pm 5.33E-04$	$0.0593 \pm 4.34E-04$	$0.0608 \pm 5.44E-04$
	75	$0.0658 \pm 6.84E-04$	$0.0660 \pm 3.95E-04$	$0.0694 \pm 2.96E-04$
	100	$0.0700 \pm 4.91E-04$	$0.0704 \pm 4.48E-04$	$0.0760 \pm 6.52E-04$
	125	$0.0729 \pm 8.56E-04$	$0.0733 \pm 7.22E-04$	$0.0814 \pm 5.03E-04$
AMAZON	25	$0.338 \pm 6.63E-04$	$0.339 \pm 6.99E-04$	$0.340 \pm 6.61E-04$
	50	$0.359 \pm 1.09E-03$	$0.360 \pm 8.04E-04$	$0.366 \pm 7.22E-04$
	75	$0.367 \pm 1.82E-03$	$0.370 \pm 1.74E-03$	$0.382 \pm 9.13E-04$
	100	$0.366 \pm 3.05E-03$	$0.371 \pm 2.53E-03$	$0.392 \pm 6.67E-04$
	125	$0.358 \pm 6.51E-03$	$0.364 \pm 4.22E-03$	$0.400 \pm 3.67E-04$
REDDIT	25	$0.0581 \pm 1.02E-03$	$0.0583 \pm 2.78E-04$	$0.0592 \pm 3.07E-04$
	50	$0.0746 \pm 1.03E-03$	$0.0738 \pm 4.85E-03$	$0.0774 \pm 7.88E-04$
	75	$0.0845 \pm 1.64E-03$	$0.0849 \pm 8.96E-04$	$0.0909 \pm 5.49E-04$
	100	$0.0904 \pm 1.35E-03$	$0.0911 \pm 1.59E-03$	$0.101 \pm 6.25E-04$
	125	$0.0946 \pm 2.13E-03$	$0.0945 \pm 3.17E-03$	$0.109 \pm 7.71E-04$

A.8.3. FIT AS A FUNCTION OF TIME

Figures 8a and 8b shows the fit as a function of time for the Amazon Reviews and NELL2 tensors. The hybrid version of CP-ARLS-LEV was used for comparison in both experiments. As in section 4.3, thick lines are averages of the running max fit across 4 ALS trials, shown by the thin dotted lines. For Amazon, the STS-CP algorithm makes faster progress than CP-ARLS-LEV at all tested sample counts.

For the NELL-2 tensor, STS-CP makes slower progress than CP-ARLS-LEV for sample counts up to $J = 163, 840$. On average, these trials with CP-ARLS-LEV do not achieve the same final fit as STS-CP. CP-ARLS-LEV finally achieves a comparable fit to STS-CP when the former uses $J = 196, 608$ samples, compared to $J = 65, 536$ for our method. Since the green curve lies completely above the light blue curve, however, we see that STS-CP makes faster progress.

These results suggest that STS-CP provides the most benefit on larger sparse tensors with high nonzero counts. With billions of nonzeros, the Amazon and Reddit tensors offset the cost of sampling in STS-CP with reductions in least-squares solve time. We can exploit the higher sample efficiency of STS-CP by dynamically changing the sample count as ALS progresses, a task that we leave for future work.